

Development of Fiber-Bundle-Image-Guided PIV

Naoki TANI*, Michitsugu MORI**, Koichi HISHIDA* and Masanobu MAEDA*

* Department of System Design Engineering, Keio University,
3-14-1 Hiyoshi, Kohoku-ku, Yokohama, Japan

** Tokyo Electric Power Co. (TEPCO), Nuclear Power Research & Development Center,
4-1 Egasaki-cho, Tsurumi-ku, Yokohama, Japan

Abstract. The present work involves the development of a particle imaging velocimetry system using an optical fiber bundle scope as shown in Figure 1. Applying a fiber scope to PIV system, the resolution of particle images is spatially poorer than those taken directly by a CCD camera, which leads to an inadequate result of cross-correlation between a pair of particle images from the fiber scope. With a conventional cross-correlation PIV, the results processed by images transmitted through a fiber scope show the direction of the vectors along the orientation of fiber elements of bundle scope, because they have a strong correlations in one frame image to the other reference frame image due to the stationary image while the particles show the intermittent images in their trace. A distribution of correlation coefficients used to obtain particle displacements has many random correlation peaks, so it is necessary to reduce background noise from the frame images. In the present study, the pattern of the fiber scope was eliminated by subtracting an initial reference image from the image with particles and using the cross-correlation PIV with a hierarchical interrogation technique could reduce erroneous vectors. Further the more improvement was tried to obtain vectors even in the case of lean particle concentration using particle streak tracking method as shown in Figure 2.

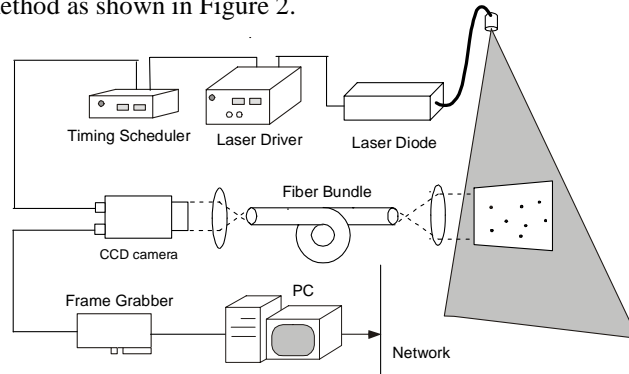


Figure 1 Fiber-Bundle-Image-Guided PIV system

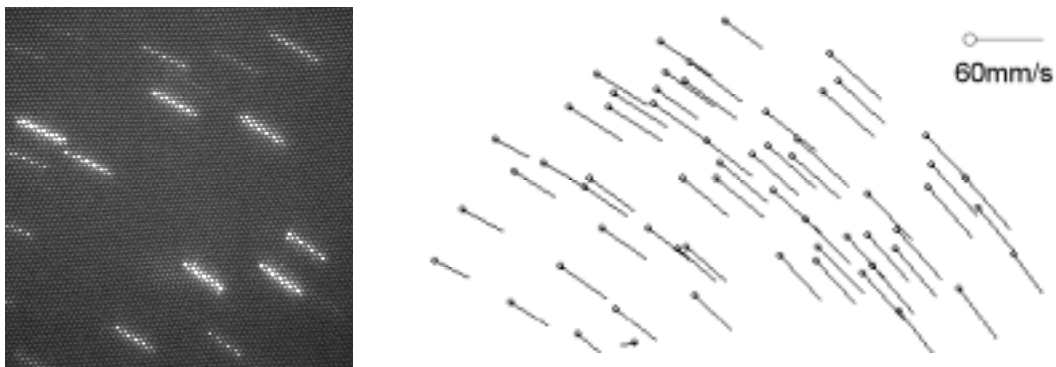


Figure 2 Particle Streak Image and Velocity Vectors

1. Introduction

Recently PIV has become a powerful tool due to its ability to provide instantaneous velocity fields (Adrian, 1991) and has contributed to highly accurate analysis of complex flows in combination with the scalar measurement of temperature and concentration (Sakakibara *et al.*, 1993). The acquisition of three-dimensional information in flow fields in order to comprehend three-dimensional phenomena is now on going research. For example, a stereoscopic system (Prasad *et al.*, 1993, Liu *et al.*, 1996) can obtain three-component velocity in a planer domain, while dual-plane PIV (Raffel *et al.*, 1996), multi-layer PIV (Abe *et al.*, 1998), and so on, can obtain three dimensional velocity fields, furthermore scanning laser sheet PIV (Brucker *et al.*, 1998) can obtain information in shallow volumetric domain by use of a high-speed camera and scanning optics.

However, when we actually investigate flows in a closed vessel such as a reactor, power plant, chemical plant, or combustor, the illumination and the recording of particle images becomes very difficult and restrictive. In these cases, it is necessary to utilize transparent optical windows in appropriate positions to observe a flow field inside a vessel. Another problem is raised where optical windows have a viewing limitation, i.e. the view is restricted to a particular angle by optical access. The optical fiber bundle scope makes it possible to thoroughly investigate a reactor since it is more flexible.

Optical fiber bundles, which can directly transmit images, are widely used in medical applications. Fiber bundles are adequately elastic, display a high, uniform light transmission capability and have an excellent heat and high radiation resistance. With these advantages, they can be effectively used for closed vessels, nuclear reactors, long pipes and so on, and are expected to become a successful diagnostic tool not only for medical applications but industrial applications such as, the visual examination of cavities.

2. Measurement system

2.1 Laser diode as illumination light source

Figure 1 shows the conceptual outline of a Fiber-Bundle-Image-Guided PIV system. A power diode laser emitting near infrared light was adopted as a light source for illumination, instead of a conventional solid-state laser as typified by Nd:YAG for PIV. Properties of this laser diode are shown in Table 1. A near infrared laser diode was designed as the high CW power and output through a fiber as is appropriate for applications in medicine, materials processing, solid-state laser pumping. The fiber-coupled linear array laser diode (SDL-3460-P6) that we adopted makes it possible to accomplish high power, compactness and portability for a PIV system. The CW powers up to 16W (shown in Figure 3)

Table 1 Properties of Laser Diode (SDL-3460-P6)

Laser Characteristics	MIN	TYP	MAX
CW Output Power	16W		17W
Center Wavelength	800nm		808nm
Spectral Width		4nm	
Threshold Current		14A	
Operating Current		32A	
Operating Voltage		2.0V	
Fiber Characteristics			
Fiber Core Diameter		600 μ m	
Fiber Numerical Aperture		0.37	

from a single multimode fiber and a numerical aperture typically less than 0.2 provides the brightness and high power density. It has a wavelength of approximately 806nm. The wavelength spectrum of the laser diode is shown in Figure 4. The output of the laser was led to an optical fiber to deliver the illuminating light. It provides simple optical access and easy handling. A laser diode can work in either a continuous wave mode or pulse mode independently of its specifications. When using the pulse mode, the chopping current carries it out generally. Figure 5 shows pulse delay characteristics of a laser diode. Emission of the laser was delayed by about 0.4msec with respect to the input voltage. An increase in diode temperature induces both reductions of output power, wavelength elongation, and shortens the life span of the diode (generally, a 10K increase of temperature results in a 50% reduction in the diode life span). It is necessary to utilize a sufficient cooling system. We adopted forced air-cooling system and its cooling power was 36W.

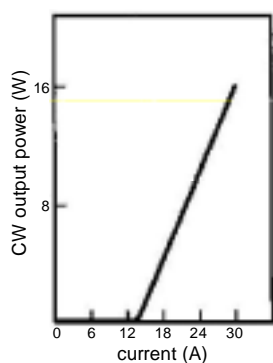


Figure 3 Light vs. Current Characteristics

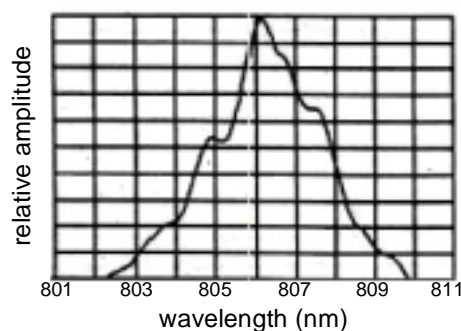


Figure 4 Wavelength Distribution of Laser Diode

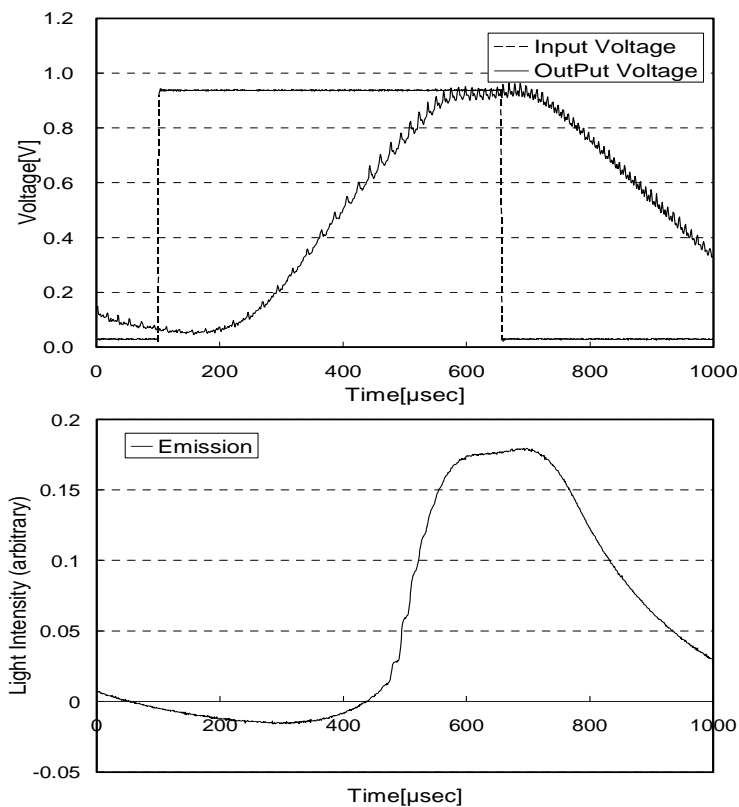


Figure 5 Pulse Delay Characteristics of Laser Diode

2.2 Recording and optical fiber bundles

A CCD camera having 640x480 pixels and a frame rate of 30Hz was attached onto the end of the fiber bundle in order to capture the images of traversing particles. The CCD camera, having a high sensitivity in the near infrared region as shown in Figure 6, was an NTSC progressive scan camera (HITACHI, KP-F2A). The non-interlaced video data of all exposed pixels are output at single-frame intervals. The computer receives the digitized images through a standard analog frame grabber board (Leutron, Picport-StereoH4D). A PCI bus equipped PC provides a sufficient transfer rate in order to capture images in real time and the frame grabber is able to transfer them directly to the system memory. After the frame grabber acquires frames, and received images are transformed into 30Hz non-interlace images by acquisition software.

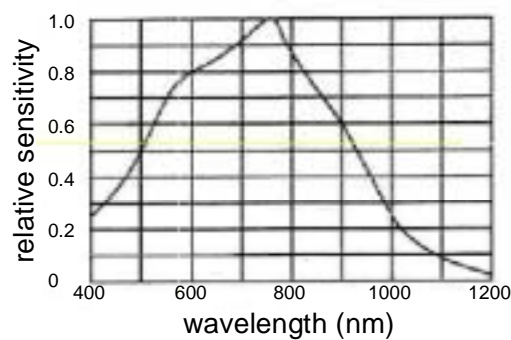


Figure 6 Spectral Sensitivity Characteristic of Near Infrared CCD Camera

Tens of thousands of optical fibers are bundled up into a fiber scope for image transmission. When both end faces are arranged with precision, an objective image can be transferred from one end to the other as shown in Figure 7. The spatial resolution is limited by the diameter of each fiber, and image quality depends on the number of bundles and the arrangement due to the lack of image at the clad of fiber core. The fibers are arranged orderly in hexagonal closed-package. If the thickness of fiber clad is small, it is likely to result in leaks of light from the fiber core. In such cases, the lines of images are blurred and contrast is reduced. Recent PIV systems employ mega-pixel CCD cameras for recording particle images, whereas the number of pixels of a fiber scope is at most 10,000-30,000 typically. An objective image is divided into 10,000-30,000 small regions and the intensity is averaged within the each fiber element. In other words, the element limits spatial resolution, which is not the case with a pixel of a CCD camera array. The fiber bundles that we adopted were of two types, 12,000 and 30,000 fibers.

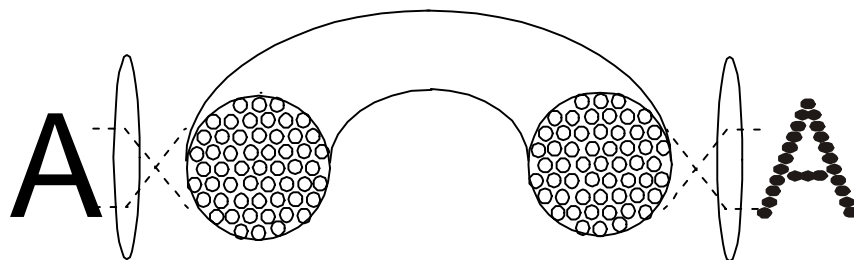


Figure 7 Directly Transformation of an Image Optical Fiber Bundle and Transferred Image of Lower Resolution

Figure 8 shows symmetric distortion, which is caused by the variations of the magnification corresponding to the object being at a distance from the optical axis. Figure 8 (b) shows the field in 40 degrees of view which can capture a larger area, but it is necessary to modify distorted images by using a least-squares polynomial technique. To correct the distortion, a calibration image was used, employing a pair of pixel coordinates in the undistorted field and pixel coordinates from a distorted calibration image. The pairs of corresponding points are calculated by cross-correlating the distorted image.

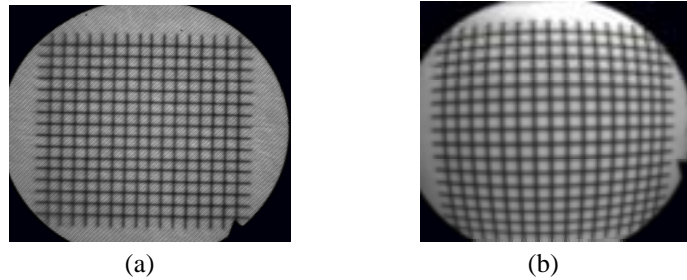


Figure 8 Distortion of Image (a) 10 degrees of view (b) 40 degrees of view

3. Experiments

3.1 Elimination of noise

Figure 9 (a) shows a partial particle image recording through a fiber scope. This particle image is of uniform flow (mean velocity was 50mm/sec). The flow channel is 100mmx100mm. This image is of lower resolution (12,000 fibers) than that of a typical CCD camera (307,200 pixels). A fiber corresponds to approximately 9-10 pixels. The image of an orderly arranged hexagonal closed-packed bundle is recorded, and also those of particles as well. They differ from conventional PIV images.

Applying a conventional cross-correlation method to particle images including arrangement of fibers, the results show the direction of the vectors along the orientation of fiber elements of the bundle scope as shown in Figure 9 (b). They have a strong correlations in one frame image to the other reference frame image due to the stationary image while the particles show the intermittent images in their trace. A pattern of the fiber array rather than a group of particles causes incorrect estimations of the correlation peak. A distribution of correlation coefficients used to obtain particle displacements has many random correlation peaks, so it is necessary to reduce background noise in particle images.

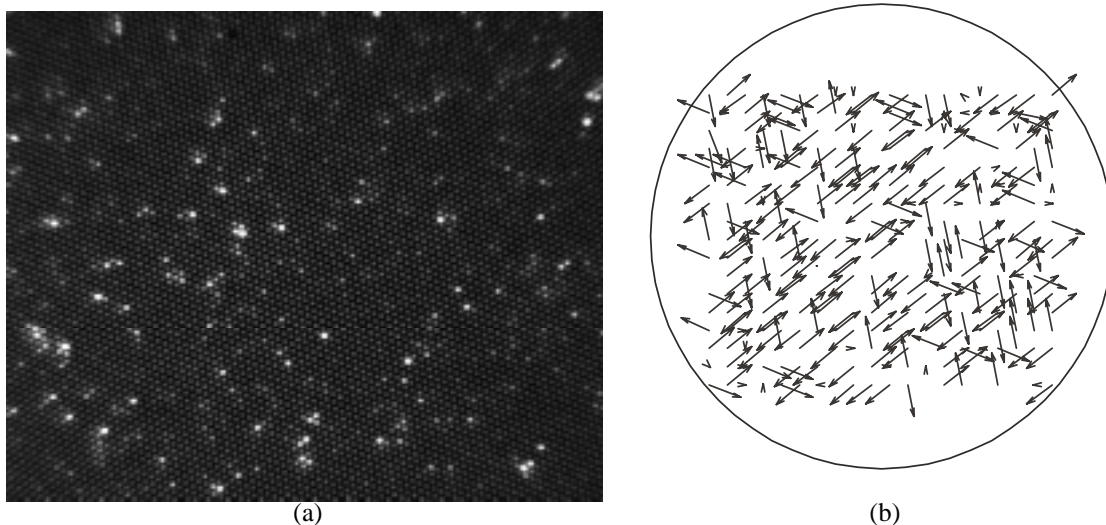


Figure 9 Partial Particle Image through a Fiber Bundle and Result of Conventional Cross-Correlation
 (a) Low Resolution Particle Image which Includes Array of Fiber Bundle
 (b) Outbreak of Erroneous Vectors, which Point in the Direction of Array of Fiber Bundle

Figure 10 (a) shows particle images being eliminated by the background image of the fiber bundle array. The system requires averages of time series intensity for every pixel, which is an image without particles. By subtracting the image without particles and referring the original image as shown in Figure 9 (a), elimination of image noise for PIV has been done. The result of elimination of a pattern of fibers is shown in Figure10 (b).The image processing method in detail is as followings.

When the recorded data (particle image including fiber bundle) is x , x can be written as;

$$x = s + n \quad (1)$$

where s represents signal (an intensity of particle), and n represents noise (an intensity of fiber bundle array). Equation (1) represented in time series data can be written as

$$x^i(k) = s^i(k) + n^i(k) \quad (2)$$

where i is the number of frame, and k is each pixel's coordinates in each frame. When the number of frames is M , the average $x(k)$ of the number of frames is written as

$$\begin{aligned} x(k) &= \frac{1}{M} \sum_{i=1}^M x^i(k) \\ &= \frac{1}{M} \sum_{i=1}^M s^i(k) + \frac{1}{M} \sum_{i=1}^M n^i(k) \end{aligned} \quad (3)$$

By averaging, an image recording only fiber bundle can be obtained. Likewise, it is possible to reduce noise images for PIV by subtracting the image without particles from the original image. In this case, 200 sheets were averaged, so the signal noise ratio was improved by 14 times as much as.

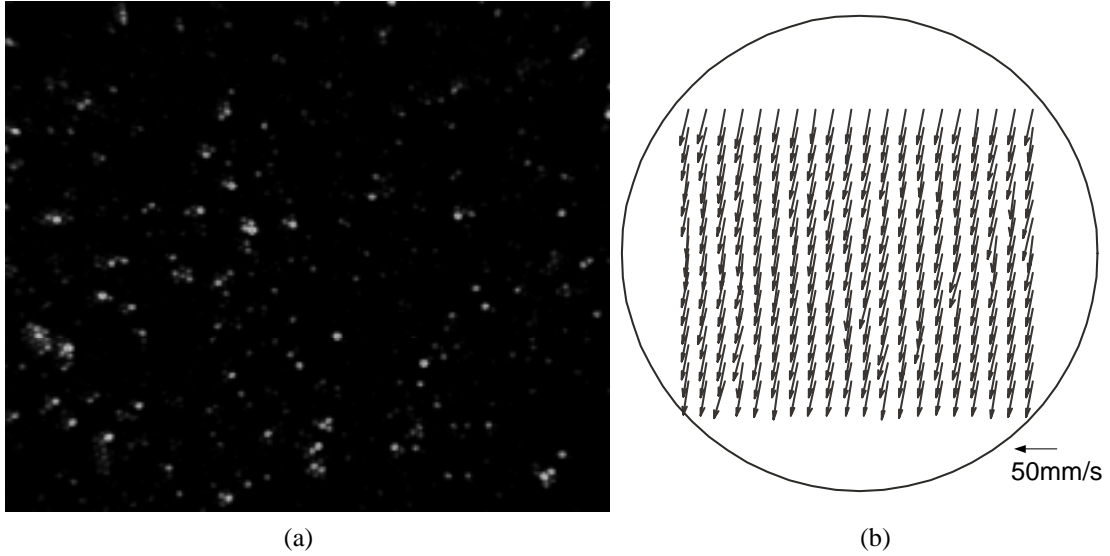


Figure 10 (a) Particle Image Eliminated a Pattern of Fibers and (b)Vector Map

3.2 Effect of fiber bundle resolution

Simulated flow field of moving particles at an angular rate (33rpm) was made by water vessel on a turntable. Polystyrene particles, 100 μ m in diameter, were seeded into a 98% glycerin solution moving on the turntable. Glycerin solution has high enough viscosity, so that the particles were fixed in the solution. Using objective lens with a 10-degree field of view, 50mm away from a laser sheet, a circle region of 14mm in diameter was observed. The measurement area was 10mm \times 10mm. The thickness of laser sheet was 2mm. The size of the reference window was 38 \times 38 pixels, which was 1.53 \times 1.53mm in real coordinates. The mean velocity vector map is shown in Figure 11.

Figure 12 shows comparisons of the results of mean velocity and rms at $x=0, y>0$ for 12K and 30K bundles of fiber. They are experimental results of rotating particles at an angular rate (33rpm) on a turntable. Mean velocities were in good agreement for those of both 12K and 30K, but in case of fluctuation, the 12K bundle results were slightly larger than those of 30K bundle. It is difficult to discern small fluctuations because of the low resolution image (12K was 4-5 pixels and 9-10 pixels). But it seems that a sort of wow on turn table was additionally contained for rms considering both 12K and 30K show similar profile.

Figure 13 shows the PDF of each velocity component at $y=5\text{mm}$. When applying the fiber bundle of 12K, dispersion was relatively larger than that of the 30K bundle. It is likely that distinguishment of the velocity fluctuation is difficult, while the mean velocity results were agreed with turn table speed.

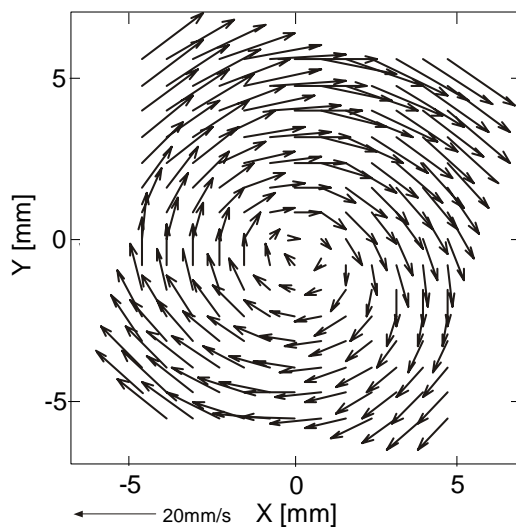


Figure 11 Mean Velocity Map of Moving Particles on a Turn Table(33rpm)

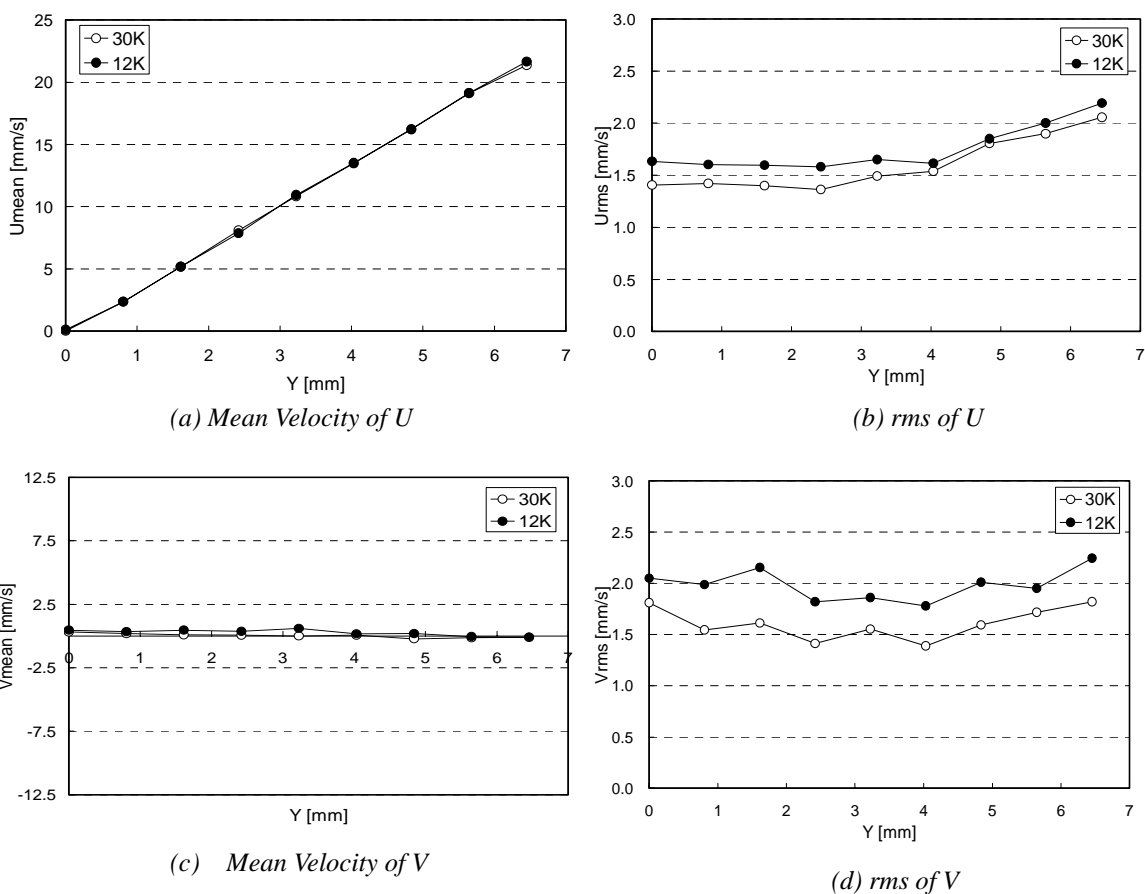


Figure 12 Mean Velocity and RMS of Cross-Correlation PIV at $X=0\text{mm}$

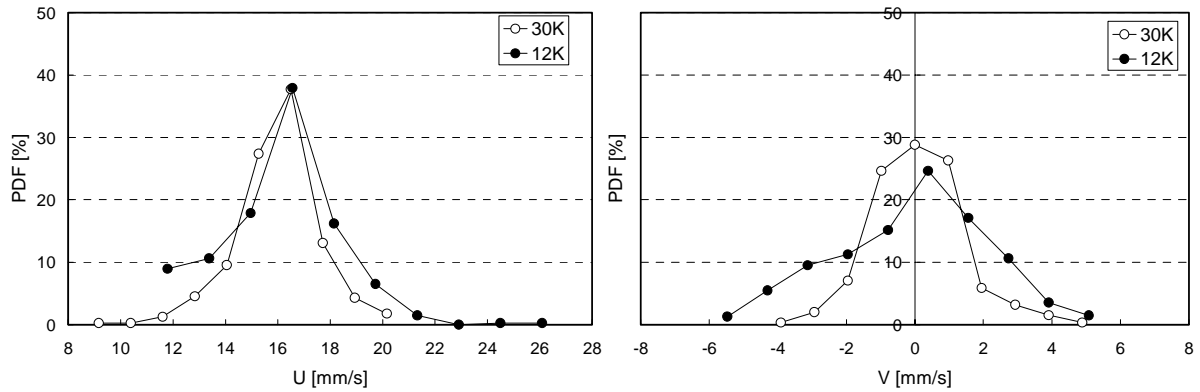
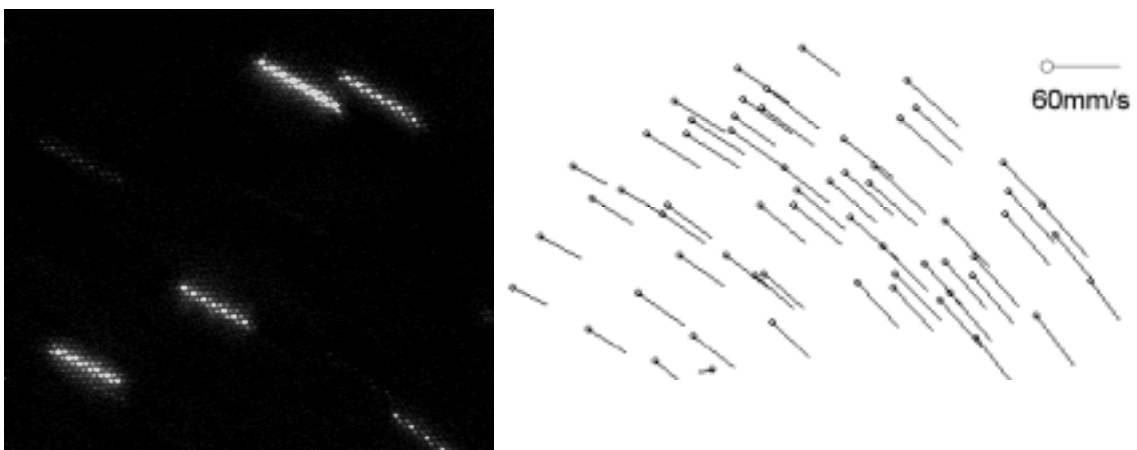


Figure 13 Probability Density Function (a)U, (b)V at Y=5mm

3.3 Particle Streak Tracking Method

In this section another approach to PIV recording is introduced. The adopted laser diode device enables us to illuminate the flow field with a certain variable durations and intervals. The incident light with appropriate duration time is shot to each frame and the camera captures path lines of particles on each frame. This is also powerful for controlling the exposure time of electrical shutter. By recording path lines of particles, we can get information for particles independent of the number of fiber bundle and the diameter of particles. The length of a path line was equivalent to several bundles of fiber, and was divided into each fiber core. This method transfers the image recording path line to binary one, labels each path line, and cross-correlates between sequential original images eliminated from the fiber bundle array. A center of reference window was located at the center of each path line. The divided path line was recognized as the same group by image processing of expansion and labeling. The reference window was 40x40 pixels which was almost the size of a path line. Figure 14 shows the partial picture of a particle streak and the results of this particle tracking method. The obtained vectors were overlapped of 60 frames of data.



(a) Particle Streak Image

(b) Velocity Vectors by Particle Tracking Method

Figure 14 Particle Streak Tracking Method

4 Conclusions

A PIV system for investigating inner flows in vessel using an optical fiber bundle has been developed and examined. The background image made by fiber bundle array affects observation, and the present system was realized for the possible applications to flow field. Additionally, the improvement of another processing technique by particle streak tracking method has been examined. A possible approach which can obtain velocity vectors independent of the number of fiber bundle was introduced.

Acknowledgement

The authors deeply acknowledge Mr. Yoshida Chief Researcher of ONO SOKKI Co.,ltd for his help on manufacturing laser diode system.

References

- Abe M., Yoshida N., Hishida K. and Maeda M., 1998, "Multi-layer PIV Technique with High Power Pulse Laser Diodes," *9th International Symposium on Applications of Laser Techniques to Fluid Mechanics, Lisbon*, 6.1
- Abe M., 1999, "Stereoscopic and multi-layer PIV system for three-dimensional flow field measurement," *M.S. Thesis, Keio University*
- Adachi T, Nishino K and Torii K, 1993, "Digital PTV measurements of a separated air flow behind a backward-facing step," *J.Flow Visualization Image Processing*
- Adrian R J, 1991, "Particle-imaging techniques for experimental fluid mechanics," *Ann, Rev. Fluid mech.*, 23, pp261-304
- Brucker C., 1998, "3-D Measurements of Bubble Motion and Wake Structure in Two-Phase Flows Using 3-D Scanning Particle-Image-Velocimetry (3-D SPIV) and Stereo-Imaging," *9th International Symposium on Applications of Laser Techniques to Fluid Mechanics, Lisbon*
- Christian Willert, 1997, "Stereoscopic digital particle image velocimetry for application in wind tunnel flows," *Meas. Sci. Technol.*, vol.8, pp1465-1479
- Gindele, Spicher, 1998, "Investigation of In-Cylinder Flow inside IC Engines Using PIV with Endoscopic Optics," *9th International Symposium on Applications of Laser Techniques to Fluid Mechanics, Lisbon*, 31.1
- Hayami H., Ohse S., Semimoto K., Ishitani T., Utsumi A., 1986, "Construction and Characteristics of Diaguide Scope"
- Liu Z C, Adrian R J, Meinhard C D, Lai W, 1996, "Structure of a turbulent boundary layer using a stereoscopic large format video-PIV, *Developments in Laser Tech. and Fluid Mech.*," 2-8, pp259-273
- Okamoto K., Hassan Y A., Schmidl W D, 1995, "New tracking algorithm for particle image velocimetry," *Exp. Fluids*, vol.19, pp342-347
- Ohmi K and Li Hang-Yu, 2000, "Particle-tracking velocimetry with new algorithms," *Meas.Sci.Technol.*, vol.11, pp603-616

- Prasad A K, Adrian R J, 1993, "Stereoscopic particle image velocimetry applied to liquid flows," *Exp.Fluids*, vol.15, pp49-60
- Raffel M., Willert C., Kompenhans J., "Particle Image Velocimetry a Practical Guide," *Springer Verlag Berlin Heideberg*
- Sakakibara J., Hishida K. and Maeda M., 1993a, "Quantitative visualization of convective heat transfer near the stagnation region of an impinging jet," *Experimental Numerical Flow Visualization*, ASME, FED-Vol. 172, pp. 93-99.
- Sakakibara J., Hishida K. and Maeda M., 1993b, "Measurement of thermally stratified pipe flow using image-processing techniques," *Experiments in Fluids*, Vol. 16, pp. 82-96.
- Soloff S M, Adrian R J, and Liu Z C, 1997, "Distortion compensation for generalized stereoscopic particle image velocimetry," *Meas. Sci. Technol.* vol.8, pp1441-1454
- Utsumi A., Kuroiwa T., Hayami H., Ohse S., Itoh A., Suzuki K., 1982, "Diaguide Scope, a new industrial fiberscope for upto 100m span